Bioorganic & Medicinal Chemistry 20 (2012) 7002–7011

Contents lists available at SciVerse ScienceDirect

Bioorganic & Medicinal Chemistry

journal homepage: www.elsevier.com/locate/bmc

Halogenated pentamethine cyanine dyes exhibiting high fidelity for G-quadruplex DNA

Rupesh Nanjunda [†], Eric A. Owens [†], Leah Mickelson, Sergey Alyabyev, Nancy Kilpatrick, Siming Wang, Maged Henary [*], W. David Wilson [*]

Department of Chemistry, Georgia State University, Atlanta, GA 30303, USA

ARTICLE INFO

Article history:
Received 21 August 2012
Revised 5 October 2012
Accepted 10 October 2012
Available online 16 October 2012

Keywords:
Cyanines
G-quadruplex
halogenation
Telomere stabilization
Surface plasmon resonance
Isothermal calorimetry
Mass spectrometry

ABSTRACT

Design and optimization of quadruplex-specific small molecules is developing into an attractive strategy for anti-cancer therapeutics with some promising candidates in clinical trials. A number of therapeutically favorable features of cyanine molecules can be effectively exploited to develop them as promising quadruplex-targeting agents. Herein, the design, synthesis and evaluation of a series of dimethylindoliene cyanine dyes with varying halogen substitutions are reported. Their interactions with telomeric and *c-myc* quadruplexes as well as a reference duplex sequence have been evaluated using thermal melting, biosensor-surface plasmon resonance, circular dichroism, isothermal titration calorimetry and mass spectrometry. Thermal melting analysis indicates that these ligands exhibit significant quadruplex stabilization and a very low duplex binding, with the dimethyl incorporation of paramount importance for decreased duplex affinity. Circular dichroism studies showed that the interaction of cyanines with quadruplex structures are primarily through stacking at one or both ends of the terminal tetrads with the two (trimethylammonium)propyl groups interacting in the accessible quadruplex grooves. Surface plasmon resonance and mass spectral studies shows the formation of an initial strong 1:1 complex followed by a significantly weaker secondary binding. Isothermal calorimetry studies show that the interaction of cyanines is predominantly entropy driven. In line with the design principles, this work provides new insights for further developing potent, highly selective cyanines as promising quadruplex-specific agents.
Published by Elsevier Ltd.

1. Introduction

It has now been convincingly demonstrated that small molecules that target quadruplexes can have cellular anticancer activity and this area is promising for new drug development.[1–4] One compound (CX-3543, Quarfloxin) has entered clinical trials with encouraging initial results against neuroendocrine cancer.[5] In spite of this success, additional quadruplex targeting compounds that display appealing pharmacodynamics with selective quadruplex binding remain highly desirable. A review of quadruplex-targeting structures illustrates a dominance of planar aromatic substituents and an overall cationic nature.[6–8] The charged groups are frequently located on a flexible chain that is linked to the aromatic system. A common binding mode for compounds displaying this motif is stacking of the aromatic moiety on the terminal tetrads of the quadruplex and the flexible cationic group(s) in one or more of the quadruplex grooves. With this model in mind, a systematic set of new cationic carbocyanines (Fig. 1) were designed and synthesized as potentially selective ligands for DNA G-quadruplexes.

Cyanine dyes have extensive applications including cancer imaging, nucleic acid detection, photographic processes, and nonlinear optical materials that utilize their outstanding photophysical properties.[9,10] Synthetic cyanines have characteristics, such as low toxicity and stability towards chemical decomposition, that make their cellular use extremely appealing. Additionally, this class of compounds displays excellent biocompatibility while being amenable to diverse chemical modifications.[9] With multiple synthetically active sites, there exist a multitude of carbocyanine dyes that can be designed and tested. Various cyanine supramolecular assemblies have been shown to probe the presence of the G-quadruplex structure in human telomere sequences.[11] Cyanine dyes have been explored as fluorescent tags to observe the three-dimensional folding properties of G-quadruplex DNA structures and dyes based on the benzothiazole heterocyclic moiety have been shown to inhibit telomerase via a suggested G-quadruplex stabilization mechanism.[12] The benzothiazole cyanines, however, generally have very strong DNA duplex minor groove interactions; therefore, a systematic set of dimethylindolenine-based pentamethine cyanine dyes

* Corresponding authors. Addresses: Georgia State University, Department of Chemistry, 100 Piedmont Avenue NE, Petit Science Center Office 315, Atlanta, GA 30303, USA. Tel.: +1 404 413 5566; fax: +1 404 413 5505 (M.H.); Department of Chemistry, Georgia State University, 50 Decatur Street, Room 540 Natural Science Center, Atlanta, GA 30303, USA. Tel.: +1 404 413 5503; fax: +1 404 413 5505 (W.D.W.).
E-mail addresses: mhenary1@gsu.edu (M. Henary), chewdw@panther.gsu.edu, wdw@gsu.edu (W. David Wilson).
† Both authors contributed equally to this work.

0968-0896/$ - see front matter Published by Elsevier Ltd.
http://dx.doi.org/10.1016/j.bmc.2012.10.008

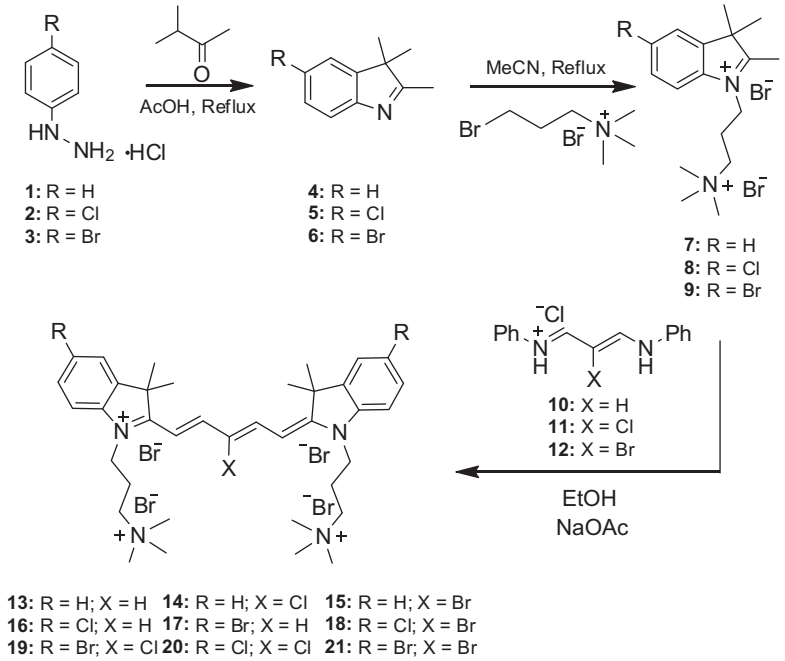

Figure 1. The synthesis of the cyanine structures used in developing G-quadruplex binding agents.

were synthesized to induce steric hindrance by the dimethyl moieties towards insertion of the compound into the duplex minor groove. Ammonium cations were introduced to the heterocyclic nitrogen to enhance solubility and increase quadruplex affinity by electrostatic interactions. Further structural diversity was achieved by halogenation at the 5-position and the *meso*-carbon of the polymethine-bridge. The interactions of these cyanine analogs with quadruplex and duplex DNA were evaluated using a variety of powerful biophysical techniques, including: DNA thermal melting screening, biosensor-surface plasmon resonance, circular dichroism, isothermal titration calorimetry and mass spectrometry. These methods reveal encouraging results as these cyanine structures bind strongly to quadruplexes with excellent selectivity over duplex DNA.

2. Results

2.1. Chemistry

In order to optimize the binding specificity and strength, we utilized the general 2,3,3-trimethylindoleline heterocyclic scaffold with heterocyclic halogenation and a 3-(trimethyl ammonium)propyl bromide substituent on the indolenine nitrogen. The synthetic pathway for obtaining the final pentamethine structures begins with Fisher-indole synthesis utilizing hydrazine derivatives **1–3** with 3-methyl-2-butanone to form modified Fischer-bases **4–6** (Fig. 1). These obtained indolenine derivatives **4–6** were alkylated with (3-bromopropyl) trimethylammonium bromide in anhydrous acetonitrile yielding dicationic salts **7–9**. Reagent **10** was commercially obtained and compounds **11** and **12** were prepared by decarboxylation of either mucochloric or mucobromic acid by aniline. Salts **7–9** were individually reacted with **10–12** in absolute ethanol under basic conditions to yield the nine corresponding tricationic pentamethine carboycyanine dyes **13–21** with varied halogen substituents.

2.2. Thermal melting (Tm)

An initial comparison of the interaction of all cyanines with Tel22 quadruplex and duplex DNA was done using UV thermal melting studies as a screening assay. Thermal melting studies were done only with the telomeric G-quadruplex because the melting temperature of *c-myc* quadruplex is too high under the currently studied salt conditions (50 mM KCl) and the changes in Tm for most of the compounds go beyond the measurable limit. The ΔTm results at ratios of cyanine to DNA ranging from 2:1 to 6:1 are shown in Table 1. The parent cyanine, compound **13**, shows a relatively low ΔTm for Tel22. Adding chlorine (**14**) or bromine (**15**) atom to the central carbon of the pentamethine chain resulted in a large increase in ΔTm with no significant difference between the Cl or Br compounds. Pentamethine cyanines with heterocyclic halogenation were then tested. Di-halogenated compounds (with terminal Cl and Br, compounds **16** and **17**, respectively) do not show any significant increase in ΔTm over the mono-substituted derivatives. The tricationic pentamethine structure was then synthesized with the incorporation of three halogen substituents (**18–21**) and these showed a substantial increase in the ΔTm with no significant difference between the Cl and Br derivatives. In summary, pentamethine cyanines with multiple halogen substituents bind to the telomeric quadruplex much more strongly than the unsubstituted parent and with very high selectivity over duplex DNA. The selectivity of these compounds is clearly very promising.

2.3. Circular dichroism (CD)

CD experiments were conducted to qualitatively evaluate the possible binding modes of the cyanine analogs with the quadruplex sequences. Achiral ligands in an unbound state do not exhibit any optical activity, however, upon complex formation with biomolecules such as DNA, they can exhibit an induced CD (ICD) signal that can be qualitatively evaluated to rationalize their binding modes.[13] As observed in duplex DNA, ligands that bind in the grooves of quadruplex motifs exhibit strong ICD signals whereas the end-stacking ligands exhibit weak ICD relative to the intensity of the DNA signal.[8,14,15] Figure 2 shows the CD plots of the parent cyanine (**13**) and the brominated analogs (**17** and **21**). The high extinction coefficients of the cyanine molecules precludes obtaining CD spectra in the compound absorption region beyond certain ligand–DNA ratios for some cyanines analogs and therefore CD

Table 1
Thermal melting studies of the cyanine analogs with telomeric quadruplex (Tel22) and a control duplex (AATT)

Compound	Tel22 (ΔTm, °C) (2:1, 4:1, 6:1 ratios)	Duplex (ΔTm, °C) (6:1 ratio)
13	2.1, 4.6, 8.7	0
14	4.6, 12.2, 13.2	2.8
15	4.6, 11.6, 15.6	0.1
16	3.1, 8.9, 13.2	0.5
17	2.5, 15.6, —[a]	1.1
18	8.0, 17.0, 20.0	1.8
19	9.0, 16.0, 21.0	2.5
20	7.0, 15.0, 19.0	2.3
21	8.0, 16.2, 20.3	1.2

The thermal melting values reported are an average of two independent trials and are reproducible within ±0.5 °C.
[a] Could not be accurately determined due to complex aggregation.

spectra only for ratios up to 3:1 are shown. All the compounds showed very weak ICD signals with Tel22 sequence as is commonly observed for ligands that stack on the terminal tetrads of quadruplex structures.[16,17] The addition of halogens did not have much effect on the magnitude and the pattern of the ICD signals suggesting a very similar end-stacking binding mode for the ligands. No changes in the DNA CD signal pattern were observed upon ligand binding suggesting the hybrid conformation of Tel22 sequence as the preferred structure for these ligands. The lack of any ICD signal with the *c-myc* sequence is also consistent with the end-stacking binding mode of the ligands (data not shown).

2.4. Surface plasmon resonance (SPR)

Biosensor-SPR studies were conducted with biotinylated, sensor-surface captured quadruplex and duplex sequences to quantitatively evaluate the binding affinity, selectivity and stoichiometry of the cyanine analogs. Figure 3 shows the SPR sensorgrams and the steady-state affinity plots for the parent compound (**13**) with the two quadruplex and reference duplex DNA sequences, and the binding affinities of all cyanine derivatives are summarized in Table 2. All the compounds exhibited an initial strong binding followed by a weaker secondary binding (ca. 5- to 50-fold) for both quadruplex sequences. The duplex binding in all the cases was too low to detect in the concentration range that was tested. The binding kinetics was rapid under the experimental conditions with both association and dissociation reactions occurring near the instrument injection mixing limit. Among the mono-substituted analogs, the bromo substitution (**15**) resulted in a slight increase in the binding affinity ($K_1 = 1.7 \times 10^6\ M^{-1}$) relative to the parent compound ($K_1 = 1.3 \times 10^6\ M^{-1}$), whereas, the chloro substitution (**14**) resulted in a decrease in the affinity with the Tel22 quadruplex. Among the symmetric, tri-substituted and mixed halogen derivatives, no improvement in the binding was observed relative to the parent compound (Table 2). The lack of an increase in affinity for the halogens, relative to the parent, as expected from the Tm results, is due to some adsorption of the halogen derivatives to the sensor surface and resulting decrease in the compound concentration. Also, dyes such as cyanines tend to aggregate in solution and this affects and reduces SPR binding affinities since the aggregated compounds must first dissociate to bind to DNA. SPR experiments were conducted in different buffer conditions to test for reproducibility and in each trial very similar value were obtained. The listed binding affinities (Table 2) are the average of two different experiments.

Interestingly, all the compounds exhibited a similar trend in the relative binding affinities with the *c-myc* quadruplex but with a significantly stronger binding (ca. 10- to 25-fold higher than the telomere) and a similar weak secondary binding. These results show a high selectivity for quadruplex sequences and confirm the selectivity observed in thermal melting studies.

2.5. Isothermal titration calorimetry (ITC)

ITC experiments were conducted by titrating all of the bromo derivatives (compounds **15**, **17** and **21**) into Tel22 and *c-myc* quadruplexes as well as the duplex model system. No significant heat change was observed in the duplex titration (not shown) in agreement with the negligible binding observed in Tm and SPR experiments. Experimental thermograms for the mono-bromo compound (**15**), are shown as examples in Figure 4 with both Tel22 and *c-myc* quadruplexes. Integrated heat versus molar ratios is also shown with the experimental results in Figure 4. The results for the *c-myc* sequence could be adequately fit with a single-site binding model over the range that could be covered in the ITC experiment. The binding with Tel22 was significantly weaker and no adequate fit to the heat versus molar ratio plot could be done over the accessible concentration range. However, it is qualitatively clear from the plot of compound **15** with Tel22 (Fig. 4A) that the binding enthalpy for Tel22 is slightly more negative than for *c-myc*. The fit values for binding enthalpy and equilibrium binding constant are given for the *c-myc* quadruplex in Table 3. From these values, the Gibbs free energy and entropy of binding were calculated and are also included in Table 3. Similar ITC results were obtained with di and tri-bromo substituted derivatives (compounds **17** and **21**) with *c-myc* quadruplex (Table 3). These results clearly

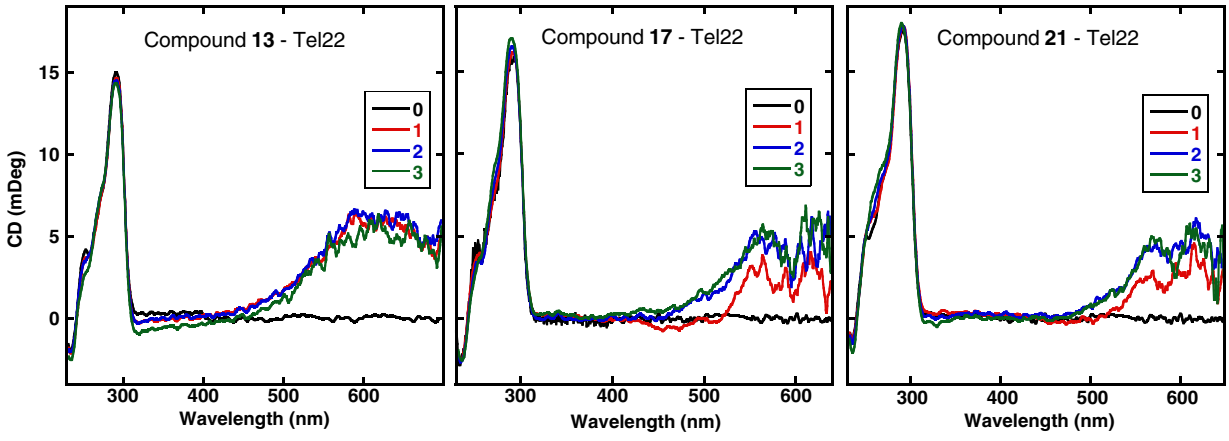

Figure 2. CD spectra of Tel22 with non-halogenated dye **13**, di-brominated (**17**) and tri-brominated analog (**21**) at 25 °C in 50 mM KCl. Single strand quadruplex concentration is 4 μM. The inset shows the ligand:quadruplex ratios.

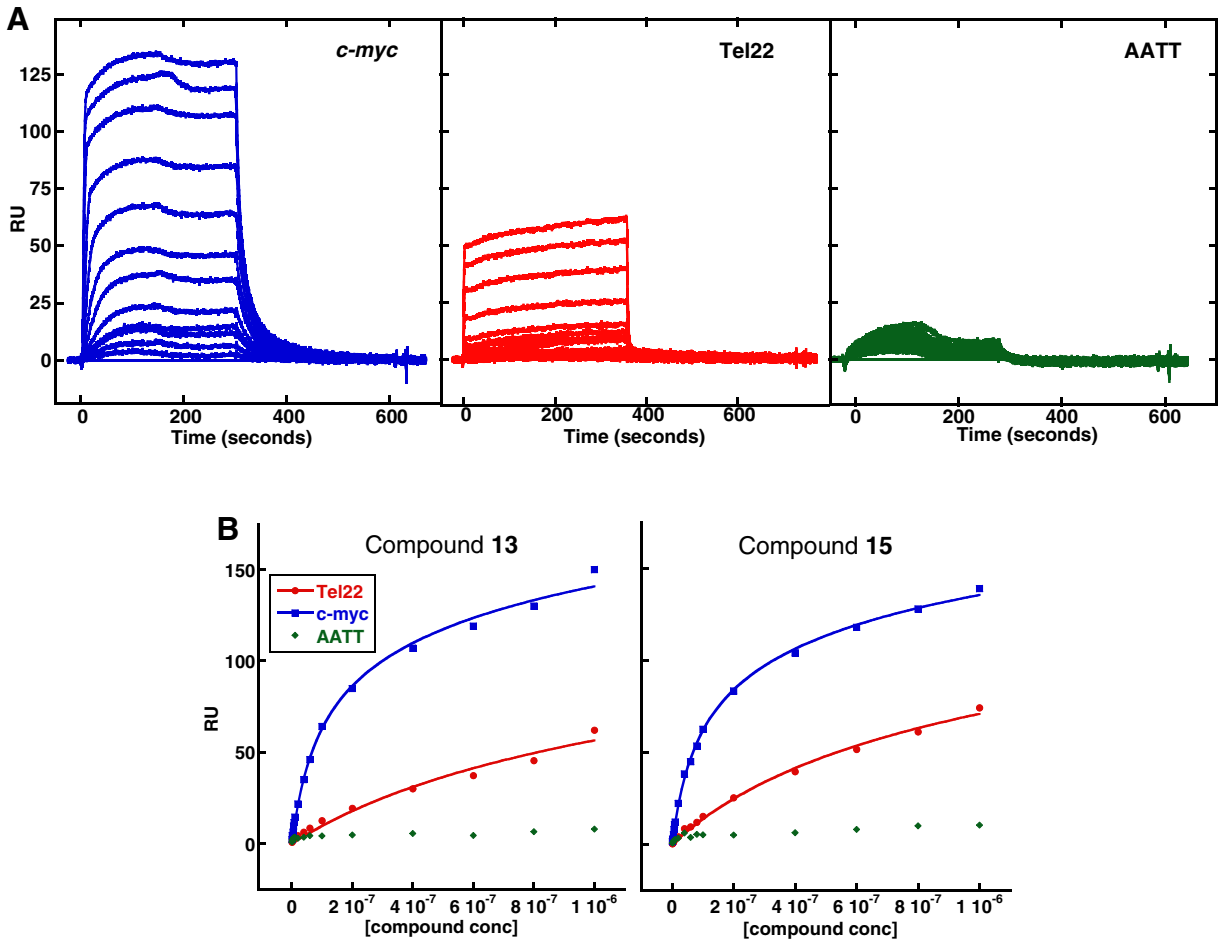

Figure 3. (A) SPR sensorgram of compound **13** with the two quadruplex as well as a reference duplex sequence. (B) Steady-state equilibrium binding plots of analogs **13** and **15**. The solid colored lines are the fits obtained using a two-site model. In all cases, the steady-state response with duplex sequence was too low to fit reasonably.

Table 2
Equilibrium binding constants of the cyanine analogs with quadruplex and duplex sequences obtained from SPR studies

Compound	Tel22 (K_1, K_2) × 10^6 M^{-1}	*c-myc* (K_1, K_2) × 10^6 M^{-1}	Duplex
13	1.3, 0.17	11.9, 0.07	$<10^5$
14	0.56, 0.08	9.7, 0.60	$<10^5$
15	1.7, 0.74	13.0, 0.07	$<10^5$
16	No binding[a]	No binding	$<10^5$
17	0.79, 0.59	5.5, 3.6	$<10^5$
18	1.0, 0.13	7.2, 0.25	$<10^5$
19	0.35, 0.05	4.8, 0.20	$<10^5$
20	0.59, 0.08	8.0, 0.23	$<10^5$
21	0.39, 0.06	9.7, 2.0	$<10^5$

The steady-state response obtained as a function of free ligand concentration was fitted to a two-site model to obtain K_1 and K_2. In all the cases, no duplex binding was observed suggesting a high selectivity of the ligands.

[a] No binding: no sensorgrams were observed in the concentration range that was tested. This might be due to the adsorption of significant amount of ligand to the sensor surface.

show that the primary driving component for binding of cyanines to *c-myc* is the entropy. As noted above the binding enthalpy is more negative for Tel22 and with a less negative ΔG of binding, the driving components for Tel22 binding will be more balanced between enthalpy and entropy.

Although ITC data was best fit with only one binding site, the SPR results suggest a weaker, second binding site. The binding heat from the primary binding site is low and the fitting results suggest that the heat is quite low for the weaker binding site, and the second site is not easily detected.

2.6. Mass spectrometry (MS)

To quantitatively and directly evaluate complex stoichiometry, mass spectrometry was done on the complexes at several compound:DNA ratios to obtain an independent determination of binding stoichiometry. Experiments were conducted with all three bromo compounds and results for compounds **13** and **15** are shown in Figure 5. For free DNA, the -4 and -5 charge species dominate and are of similar magnitude. On addition of the compound, a 1:1 complex peak can be seen. As the ratio is increased, the 1:1 peak grows in intensity and a smaller 2:1 peak can be seen at higher ratios. It is clear from the mass spectrometry results that the binding is a two site non-cooperative interaction in agreement with the SPR analysis.

3. Discussion

The discovery of G-quadruplex structures and their potential involvement in important biological pathways as well as cancer development has significantly extended our understanding of the importance of non-B-form DNA structures in cellular function. In addition, such non-B structures can provide an alternate platform for developing structure-specific small molecules as part of a new therapeutic approach. To use the DNA quadruplex structure

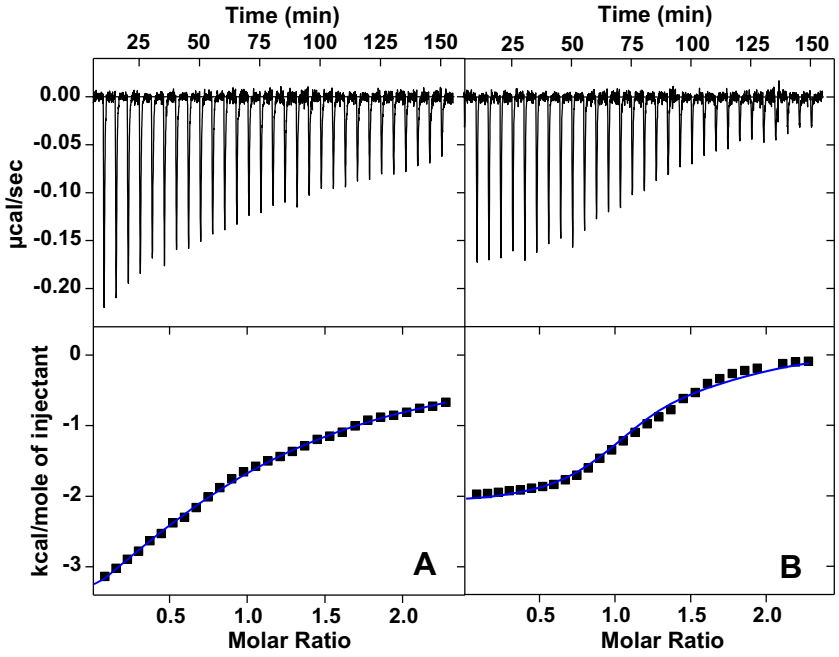

Figure 4. ITC thermograms of the mono-bromine compound **15** with Tel22 (A) and *c-myc* (B) sequences. Raw heats are displayed in top panels, while the corrected, integrated plots are in the bottom panel. The solid blue lines represent the fit obtained using a single-site model, and the thermodynamic parameters are shown in Table 3.

Table 3
Thermodynamic parameters for the bromine analogs with *c-myc* quadruplex sequence derived from ITC and SPR studies

Compound	ΔH (kcal/mol)	ΔG (kcal/mol)	$T\Delta S$ (kcal/mol)	*n*
15	−2.1	−9.8	7.7	1.2
17	−1.9	−9.3	7.3	0.98
21	−3.6	−9.6	6.0	0.91

The intergrated heats were fit to a single-site model using the primary binding constant values (K_1) from SPR to obtain the enthalpy values. ΔG was calculated using $\Delta G = -RT\ln K_1$ and $T\Delta S$ using $\Delta G = \Delta H - T\Delta S$.

as a platform for anticancer drug development, it is essential to design and discover new agents that can discriminate between quadruplex and duplex structures with very high selectivity. Furthermore, the diversity of quadruplex conformations found in the genome also makes the development of ligands that can discriminate between different quadruplex folds quite attractive.[2,18,19] The dimethylindolenine cyanine scaffold was selected based on the concepts that it could not fit into the minor groove, as with planar cyanines, but could stack on the terminal tetrads of quadruplex structure with cationic chains in the quadruplex grooves. A survey of all the approved drugs that are currently being used, as well as drug candidates that are in clinical development, shows that a majority of the drugs have halogen atoms incorporated to increase the pharmacological properties of the drug molecule.[20–22] While fluorine and chlorine are the most prevalent halogens used, brominated drugs can also increase the desired pharmacological features.[23] With this in mind for an initial test series, coupled with a number of features of cyanine molecules that are considered to be therapeutically favorable, a series of pentamethine-bridged cyanine analogs with various combinations of chlorine and bromine substitutions on the core aromatic system as well as on the meso-carbon of the pentamethine chain were synthesized. Their quadruplex binding potential and selectivity over duplex binding were evaluated using a complementary series of biophysical techniques.

The initial screening with thermal melting showed a very high selectivity by all the cyanine analogs for the quadruplex over duplex structures. This very promising finding is consistent with the design principles aimed at the development of strong quadruplex and weaker duplex binding. The thermal stability of the quadruplex sequence further increased with the addition of halogens and the tri-halogenated analogs inducing the highest stability. The introduction of either chlorine or bromine clearly increased the stabilization potential as compared to the parent molecule, however, no significant difference in the thermal melting values were found between the Cl or Br analogs as they both bound strongly to quadruplexes. The presence of polar atoms such as chlorine and bromine clearly has a positive and an additive effect on the binding to the quadruplex sequence. The lack of significant selectivity between Cl and Br suggests that the unfavorable steric contributions are minimal for these substitutions. Furthermore, the presence of two bulky methyl groups on both aromatic rings provides a steric hindrance to minimize binding to the duplex sequence.

Circular dichroism analysis indicates predominant end-stacking and much weaker groove interactions for all the ligands with quadruplex structures, based on the presence of weak ICD signals in the compound absorbance region upon complex formation. Weak ICD is a commonly observed pattern for ligands that either intercalate with duplex sequences[24,25] or stack on the terminal tetrads of quadruplex motifs with weak groove interactions.[14] The two 3-(trimethylammonium)propyl substituents on these cyanine systems (Fig. 1) can favorably interact with the accessible grooves of the quadruplex. The secondary binding observed in SPR might be due to the weak interactions of a second ligand in the quadruplex grooves resulting in ICD signals of low magnitude. The lack of any CD changes in the DNA region of the spectra further indicates the native conformation as the preferred quadruplex binding conformer for the cyanine analogs. Human telomeric quadruplex can adopt different quadruplex folds under solution conditions and these different folds have been shown to exist in equilibrium due to a low energy barrier between them.[24–26] Various small molecules have been designed and developed that can target different

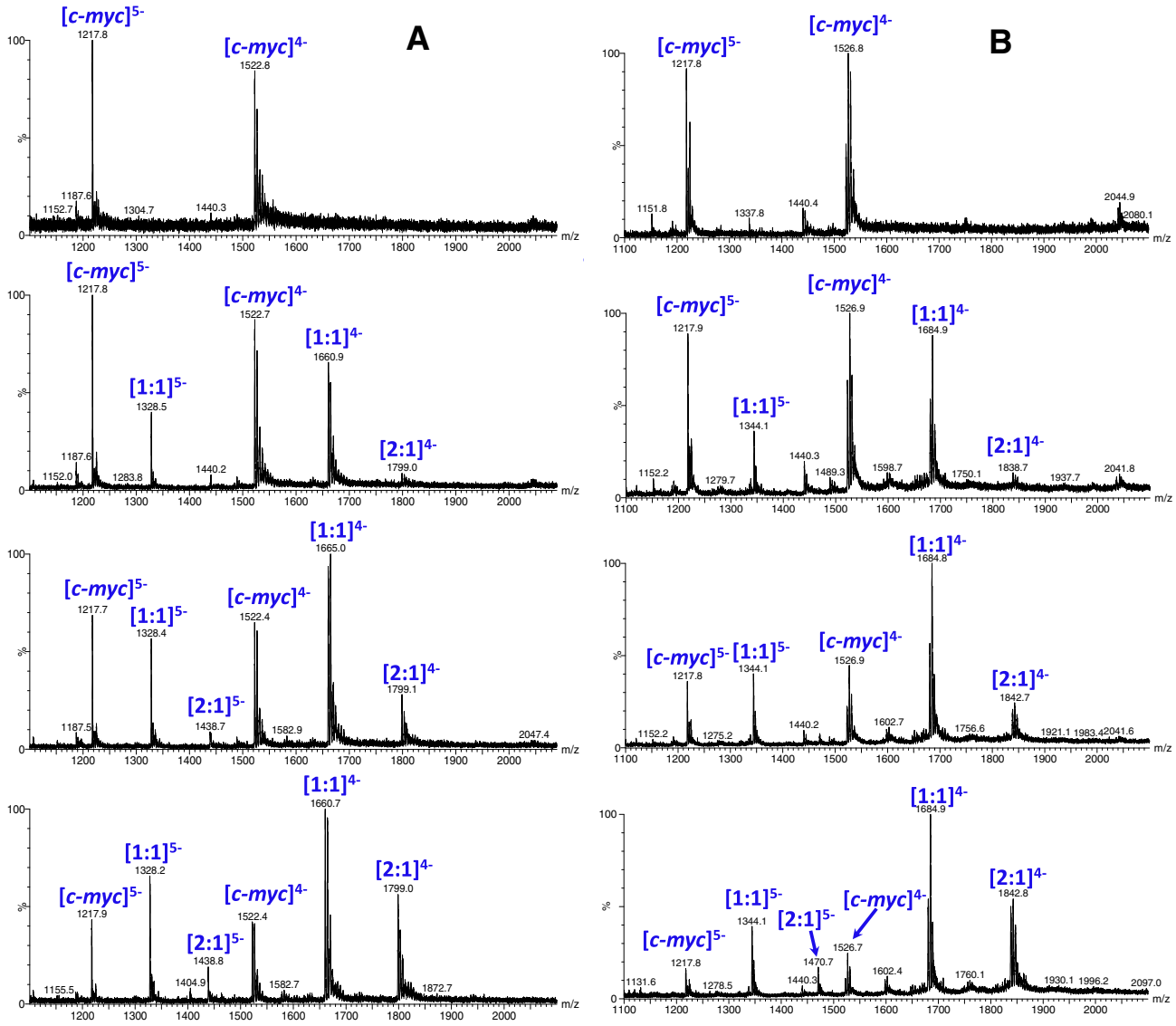

Figure 5. Mass spectra of *c-myc* quadruplex with 0:1, 1:1, 2:1, 4:1 ratios (top to bottom) of parent dye **13** (A) and mono-brominated compound **15** (B).

folds of telomeric quadruplex as well as small molecules that can facilitate the interconversion between different conformers upon binding.[14,17,27–29] In almost all cases, ligand induced conformational changes upon binding is a commonly observed phenomena. The different conformations of the telomeric quadruplex does not necessarily alter the ligand binding mode because of the very small energy required to induce the interconversion between different folds without changing the mode of binding for the ligand. From the CD results, the lack of any significant changes in the DNA spectral region indicates that the native hybrid conformation of the telomeric quadruplex is the preferred quadruplex conformer for the cyanine analogs.

CD results are further supported by the presence of an initial strong binding site detected by SPR studies. The two-site model predicted an initial strong binding that can be attributed to end-stacking and a significantly weaker secondary binding. Interestingly, all the compounds exhibited a 10-fold higher affinity for the *c-myc* quadruplex over the telomeric quadruplex. This can be due to the structural differences between the quadruplex folds from *c-myc* and telomeric sequence. The *c-myc* sequence folds into a single, highly stable parallel architecture where all the strands are parallel to each other and the connecting loops run diagonally along the grooves of the quadruplex. In such a parallel architecture, both the terminal tetrads of the quadruplex are completely exposed without any steric hindrance from the loop nucleobases, and therefore the exposed surface of terminal tetrads are highly conducive for favorable ligand stacking. Telomeric quadruplex, however, can fold into a multitude of conformers in solution with the hybrid conformation as the predominant fold. The two lateral TTA loops of the hybrid fold run across the terminal tetrads on both ends, and therefore the highly dynamic nucleobases of the loop render some steric hindrance for effective ligand stacking resulting in decreased binding affinities for telomeric quadruplex as compared to *c-myc*.

The stoichiometry analysis was strongly supported by the mass spectral results where the formation of a predominant 1:1 complex species and a weaker 2:1 complex was observed. ITC thermodynamic analysis of cyanine–quadruplex interactions revealed a predominantly entropy driven complex formation with *c-myc* quadruplex. Although the binding enthalpy largely remained the same for the mono- and di-bromo additions, the tri-bromo analog showed a favorable increase in enthalpy (ca. twofold), owing to the

larger van der Waals interactions due to the additional bromine. It also had a corresponding small decrease in entropy, probably due to the conformational restriction imposed by the bulky bromine addition upon complex formation.

4. Conclusions

In conclusion, a series of halogenated cyanine dyes were systematically designed, synthesized and tested for their interaction potential with quadruplex sequences using complementary lines of biophysical techniques. In conjunction with the design principles, to enhance quadruplex specificity with low duplex affinity, several of the cyanine analogs in this study showed elevated binding to both telomeric and *c-myc* quadruplex structures while maintaining a very low duplex selectivity. The dimethyl incorporation on both indolenine rings provide the necessary steric hindrance for the cyanine moiety to decrease duplex groove interactions, while the more polar halogen substitutions enhanced quadruplex binding. Thermal melting studies showed a relative increase in quadruplex stability as the number of halogen substitutions was increased. The small ICD signal observed upon complex formation indicates that the cyanines are interacting with the quadruplex structure primarily through end-stacking mode. The formation of a strong 1:1 complex as observed in SPR and mass spectral studies further supports the end-stacking binding mode of the ligands. The currently designed ligands provide the necessary platform in developing further potent cyanine molecules as promising quadruplex-specific agents.

5. Experiments

5.1. Pentamethine dye synthesis

Sigma–Aldrich or TCI America were the commercial sources for the starting materials utilized in the presented synthesis and the reagents were used without purification. The ^{1}H NMR and ^{13}C NMR spectra were recorded on a Bruker Avance (400 MHz) spectrometer using DMSO-d_6 or MeOD-d_4 containing tetramethylsilane (TMS) as an internal calibration standard. UV–Vis/NIR absorption spectra were recorded on a Varian Cary 50 spectrophotometer. High-resolution accurate mass spectra (HRMS) were obtained either at the Georgia State University Mass Spectrometry Facility using a Waters Q-TOF micro (ESI-Q-TOF) mass spectrometer or utilizing a Waters Micromass LCT TOF ES+ Premier Mass Spectrometer. Liquid chromatography (LC) utilized a Waters 2487 single wavelength absorption detector with wavelengths set between 640 and 700 nm depending on the dye's photophysical properties. The column used in LC was a Waters Delta-Pak 5 μM 100A 3.9 × 150 mm reversed phase C_{18} column. Evaporative light scattering detection analyzes trace impurities that cannot be observed by alternate methods; a SEDEX 75 ELSD was utilized in tandem with liquid chromatography to observe and confirm purity.

5-Chloro-2,3,3-trimethyl-3H-indole (**5**) and *5-Bromo-2,3,3-trimethyl-3H-indole* (**6**) were prepared using the procedure published by Zimmermann et al.[6] They were obtained as reddish brown oils in 71% and 90% yield, respectively.

5.1.1. General synthetic procedure for preparation of heterocyclic salts

A mixture of corresponding indole derivative **4–6** (31.4 mmol) and 3-bromopropyl trimethylammonium bromide (9.0 g, 34.5 mmol) was refluxed for 72 h in anhydrous acetonitrile (100 mL) under nitrogen. The reaction was cooled to room temperature and solid product precipitated after 4 h. The precipitate was filtered and was washed with acetone and diethyl ether.

2,3,3-Trimethyl-1-(3-(trimethylammonio)propyl)-3 *H-indol-1-ium* bromide (**7**) was synthesized by our group and is previously reported.[7]

5.1.1.1 5-Chloro-2,3,3-trimethyl-1-(3-(trimethylammonio) propyl)-3H-indol-1-ium bromide (8). Yield 82%; mp 215–217 °C; ^{1}H NMR (400 MHz, DMSO-d_6), δ: 1.65 (s, 6H), 2.56 (t, J = 8.0 Hz, 2H), 3.25 (s, 9H), 3.73 (tt, J = 8.0 Hz, J = 8.0 Hz, 2H), 4.64 (t, J = 8.0 Hz, 2H), 4.80 (s, 3H), 7.69 (dd, J = 8.8 Hz, J = 2.0 Hz, 1H), 7.84–7.92 (m, 2H); ^{13}C NMR (100 MHz, DMSO-d_6): δ 12.2, 20.0, 20.7, 43.3, 52.1, 53.2, 61.5, 115.9, 123.3, 128.8, 134.3, 138.2, 142.3, 197.9. Composition in theory: C(44.91%), H(5.99%), N(6.16%); Composition found: C(45.01%), H(6.29%), N(6.08%); HRMS (ESI) calculated for $[C_{17}H_{27}ClN_2]^{2+}$ m/z 147.4356, found m/z 146.9909, 148.0421

5.1.1.2. 5-Bromo-2,3,3-trimethyl-1-(3-(trimethylammonio) propyl)-3*H*-indol-1-ium bromide (9). Yield 81%; Mp 225–227 °C; ^{1}H NMR (400 MHz, DMSO-d_6), δ: 1.57 (s, 6H), 2.27 (s, 9H), 3.02 (s, 3H), 3.83 (t, J = 8.0 Hz, 2H), 4.57 (t, J = 8.0 Hz, 2H), 7.61 (m, 2H), 7.88 (t, J = 5.6 Hz, 1H). ^{13}C NMR (100 MHz, DMSO-d_6): δ 15.2, 22.0, 25.5, 30.6, 52.3, 54.3, 63.9, 115.6, 123.5, 128.8, 129.3, 140.9, 141.7, 197.7. Composition in theory: C(40.91%), H(5.45%), N(5.61%); Composition found: C(40.84%), H(5.48%), N(5.94%); HRMS (ESI) calculated for $[C_{17}H_{27}BrN_2]^{2+}$ m/z 169.6611, found m/z 169.7002.

5.1.2. General synthetic procedure for the preparation of methine bridge reagent

(E)-N-((Z)-2-Chloro-3-(phenylamino)allylidene) benzenaminium chloride (**11**) was synthesized using the reported procedure.[30] 88% yield; Mp 214–216 °C.

5.1.2.1. (*E*)-*N*-((*Z*)-2-Bromo-3-(phenylamino)allylidene) benzenaminium chloride (12). Mucobromic acid (5.940 g, 23.04 mmol) was dissolved in ethanol (40 mL) and aniline (4.286 g, 4.2 mL, 46.1 mmol), diluted with ethanol (20 mL), was added dropwise over a 10-min period. The reaction vessel was under vigorous stirring and was gently heated to 40 °C. After the addition of aniline was finished, $CO_{2(g)}$ was further produced indicating the reaction was not complete. Upon completion of $CO_{2(g)}$ evolution, the golden brown reaction mixture was cooled in an ice bath. Diethyl ether (50 mL) was added slowly at reduced temperature under heavy stirring until a bright yellow solid precipitated. The resulting solid was filtered, washed with ether, dried and was used without purification in subsequent reactions. Yield 75%; Mp 189–191 °C; ^{1}H NMR (400 MHz, DMSO-d_6): δ 7.330 (t, J = 7.2 Hz, 2H), 7.496 (t, J = 8 Hz, 4H), 7.708 (d, J = 8 Hz, 4H), 9.559 (s, 2H), 11.513 (s, 2H); ^{13}C NMR (100 MHz, DMSO-d_6): δ 89.3, 119.5, 123.9, 126.0, 129.2, 129.6, 138.5, 157.4.

5.1.3. General procedure for obtaining tricationic pentacarbocyanines 13–21

A mixture of individual salts **7–9** (2 equivalents), either malonaldehyde bisphenylimine monohydrochloride **10**, chlorinated analog **11** or brominated analog **12** (1 equiv) and sodium acetate (3 equiv) were refluxed for 6 hrs in anhydrous ethanol under nitrogen atmosphere and then cooled to room temperature. The reaction mixture was concentrated in vacuo. The crude product was dissolved in deionized water and the target compounds **9–12** were isolated using silica gel 40–63 μm 90 Å C_{18} reversed phase column chromatography using 20% methanol in water as eluting solvent.

5.1.3.1. 2-((1*E*,3*E*,5*E*)-5-(3,3-Dimethyl-1-(3-(trimethylammonio)-propyl)indolin-2-ylidene)penta-1,3-dien-1-yl)-3,3-dimethyl-1-(3-(trimethylammonio)propyl)-3H-indol-1-ium bromide (13). Yield 71%; Mp 218–221 °C; ^{1}H NMR (400 MHz, MeOD-d_4): δ 1.781 (s, 12H), 2.359–2.380 (m, 4H), 3.248 (s, 18H), 3.750 (t, J = 8.4 Hz, 4H), 4.254 (t,

J = 7.6 Hz, 4H), 6.628 (d, J = 13.6 Hz, 2H), 7.140 (t, J = 12.4 Hz, 1H), 7.287–7.327 (m, 2H), 7.436–7.486 (m, 4H), 7.540 (d, J = 7.6 Hz, 2H), 8.345 (t, J = 13.2 Hz, 2H); ^{13}C NMR (400 MHz, MeOD-d_4): δ 20.93, 26.56, 40.26, 49.22, 52.49, 63.08, 103.72, 110.41, 122.20, 125.07, 127.11, 128.50, 141.23, 141.76, 154.80, 173.47. High-resolution electrospray ionization (ESI) accurate mass spectra calculated m/z for $[C_{37}H_{55}N_4Br_2]^+$ 713.2793, found 713.2767.

5.1.3.2. 2-((1*E*,3*Z*,5*E*)-3-Chloro-5-(3,3-dimethyl-1-(3-(trimethylammonio)propyl)indolin-2-ylidene)penta-1,3-dien-1-yl)-3,3-dimethyl-1-(3-(trimethylammonio)propyl)-3H-indol-1-ium bromide (14). Yield 46%; Mp 225–227 °C; ^{1}H NMR (400 MHz, DMSO-d_6): δ 1.81 (s, 12H), 2.40 (t, J = 7.4 Hz, 4H), 3.26 (s, 18H), 3.71–3.79 (m, 4H), 4.38 (t, J = 7.6 Hz, 4H), 6.55 (d, J = 13.4 Hz, 2H), 7.36 (t, J = 7.2 Hz, 2H), 7.50 (t, J = 7.6 Hz, 2H), 7.58 (d, J = 7.6 Hz, 2H), 7.63 (d, J = 7.6 Hz, 2H), 8.50 (d, J = 13.4 Hz, 2H); ^{13}C NMR (100 MHz, DMSO-d_6), δ: 20.9, 26.0, 40.7, 49.4, 52.5, 63.0, 100.9, 111.9, 122.2, 123.2, 125.6, 128.6, 141.4, 141.7, 148.2, 175.1. Composition in theory: (x3H_2O): C (50.27%), H (6.84%), N (6.34%); Composition found: C (50.16%), H (6.78%), N (6.26%); HRMS (ESI) calculated for $[C_{37}H_{54}ClN_4]^{3+}$ m/z 197.1331, found m/z 197.1337.

5.1.3.3. 2-((1*E*,3*Z*,5*E*)-3-Bromo-5-(3,3-dimethyl-1-(3-(trimethylammonio)propyl)indolin-2-ylidene)penta-1,3-dien-1-yl)-3,3-dimethyl-1-(3-(trimethylammonio)propyl)-3H-indol-1-ium bromide (15). Yield 66%; Mp 174–176 °C; ^{1}H NMR (400 MHz, DMSO-d_6): δ 1.77 (s, 12H), 2.31 (t, J = 7.1 Hz, 4H), 3.13 (s, 18H), 3.58–3.68 (m, 4H), 4.34 (t, J = 7.0 Hz, 4H), 6.40 (d, J = 13.2 Hz, 2H), 7.61 (d, J = 8.6 Hz, 2H), 7.76 (d, J = 8.6 Hz, 2H), 8.11 (s, 2H), 8.61 (d, J = 13.2 Hz); ^{13}C NMR (100 MHz, DMSO-d_6), δ: 22.4, 27.6, 42.2, 51.8, 54.0, 64.2, 112.3, 118.3, 123.2, 127.1, 130.8, 143.6, 151.3, 176.1. Composition in theory: C (50.82), H (6.22), N (6.41); Composition found: C (50.48), H (6.75), N (6.45). High-resolution electrospray ionization (ESI) accurate mass spectra calculated m/z for $C_{37}H_{54}N_4Br_2$ 712.2715, found 712.2722.

5.1.3.4. 5-Chloro-2-((1*E*,3*E*,5*E*)-5-(5-chloro-3,3-dimethyl-1-(3-(trimethylammonio)propyl)indolin-2-ylidene)penta-1,3-dien-1-yl)-3,3-dimethyl-1-(3-(trimethylammonio)propyl)-3H-indol-1-ium bromide (16). Yield 88%; ^{1}H NMR (400 MHz, MeOD-d_4): δ 1.78 (s, 12H), 2.32 (s, 4H), 3.25 (s, 18H), 3.75 (t, J = 8.4 Hz, 4H), 4.24 (t, J = 7.6 Hz, 4H), 6.60 (d, J = 13.2 Hz, 2H), 7.11 (t, J = 12.4 Hz, 1H), 7.50–7.43 (m, 4H), 7.58 (s, 2H), 8.35 (t, J = 13.2 Hz, 2H). ^{13}C NMR (400 MHz, MeOD-d_4): δ 20.89, 26.50, 40.58, 49.35, 52.57, 63.05, 104.20, 111.92, 122.72, 127.75, 128.49, 130.54, 140.59, 143.15, 155.05, 173.28. High-resolution electrospray ionization (ESI) accurate mass spectra calculated m/z for $[C_{37}H_{53}N_4Cl_2]^{3+}$ 207.7877 found 207.7755.

5.1.3.5. 5-Bromo-2-((1E,3E,5E)-5-(5-bromo-3,3-dimethyl-1-(3-(trimethylammonio)propyl)indolin-2-ylidene)penta-1,3-dien-1-yl)-3,3-dimethyl-1-(3-(trimethylammonio)propyl)-3H-indol-1-ium bromide (17). Yield 62%; Mp 237–240 °C; ^{1}H NMR (400 MHz, MeOD-d_4): δ 1.782 (s, 12H), 2.318 (t, J = 7.1 Hz, 4H), 3.241 (s, 18H), 3.707–3.750 (m, 4H), 4.224 (t, J = 7.2 Hz, 4H), 6.642 (d, J = 13.6 Hz, 2H), 7.176 (t, J = 12.8 Hz, 1H), 7.384 (d, J = 8.4 Hz, 2H), 7.611 (d, J = 8.4 Hz, 2H), 7.735 (s, 2H), 8.362 (t, J = 12.8 Hz, 2H); ^{13}C NMR (400 MHz, MeOD-d_4): δ 20.89, 26.06, 26.50, 40.55, 49.32, 52.60, 63.03, 104.27, 112.25, 117.93, 125.63, 131.45, 141.04, 143.44, 155.07, 173.11 High-resolution electrospray ionization (ESI) accurate mass spectra calculated m/z for $[C_{37}H_{52}N_4Br_2]^+$ 710.2559, found 710.2552.

5.1.3.6. 2-((1*E*,3*Z*,5*E*)-3-Bromo-5-(5-chloro-3,3-dimethyl-1-(3-(trimethylammonio)propyl)indolin-2-ylidene)penta-1,3-dien-1-yl)-5-chloro-3,3-dimethyl-1-(3-(trimethylammonio)propyl)-3H-indol-1-ium bromide (18). Yield 88%; Mp 238–240 °C; ^{1}H NMR (400 MHz, DMSO-d_6): δ 1.77 (s, 12H), 2.19 (t, J = 7.6 Hz, 4H), 3.13 (s, 18H), 3.63 (tt, J = 7.6 Hz, J = 7.8 Hz, 4H), 4.25 (t, J = 7.8 Hz, 4H), 6.34 (d, J = 13.4 Hz, 2H), 7.53 (d, J = 8.0 Hz, 2H), 7.68 (d, J = 8.0 Hz, 2H), 7.94 (s, 2H), 8.61 (d, J = 13.4 Hz, 2H); ^{13}C NMR (400 MHz, DMSO-d_6), δ: 18.5, 20.6, 26.4, 41.4, 49.8, 52.3, 62.2, 102.7, 113.3, 117.0, 123.2, 128.3, 130.1, 140.5, 143.4, 150.3, 174.4. Composition in theory: (x3H_2O): C (44.56%), H (5.86%), N (5.62%); Composition found: C (44.54%), H (5.78%), N (5.56%); HRMS (ESI) calculated for $[C_{37}H_{52}Br_2Cl_2N_4]^+$ m/z 780.1936, found 780.1916.

5.1.3.7. 5-Bromo-2-((1E,3Z,5E)-5-(5-bromo-3,3-dimethyl-1-(3-(trimethylammonio)propyl)indolin-2-ylidene)-3-chloropenta-1,3-dien-1-yl)-3,3-dimethyl-1-(3-(trimethylammonio)propyl)-3H-indol-1-ium bromide (19). Yield 80%; Mp 227–229 °C; ^{1}H NMR (400 MHz, DMSO-d_6): δ 1.76 (s, 12H), 2.17 (t, J = 7.0 Hz, 4H), 3.12 (s, 18H), 3.58–3.68 (m, 4H), 4.26 (t, J = 6.8 Hz, 4H), 6.35 (d, J = 13.4 Hz, 2H), 7.61 (d, J = 8.6 Hz, 2H), 7.65 (d, J = 8.6 Hz, 2H), 8.05 (s, 2H), 8.56 (d, J = 13.4 Hz, 2H); ^{13}C NMR (400 MHz, DMSO-d_6), δ: 20.7, 26.4, 41.2, 49.7, 52.3, 62.2, 100.3, 113.7, 118.1, 123.5, 126.0, 131.3, 140.4, 143.5, 148.7, 174.9. Composition in theory: (x3H_2O): C (42.65%), H (5.61%), N (5.38%); Composition found: C (42.09%), H (5.80%), N (5.26%); HRMS (ESI) calculated for $[C_{37}H_{52}Br_2ClN_4]^+$ m/z 745.2247, found m/z 745.2255.

5.1.3.8. 5-Chloro-2-((1E,3Z,5E)-3-chloro-5-(5-chloro-3,3-dimethyl-1-(3-(trimethylammonio)propyl)indolin-2-ylidene)penta-1,3-dien-1-yl)-3,3-dimethyl-1-(3-(trimethylammonio)propyl)-3H-indol-1-ium bromide (20). Yield 77%; Mp 222–224 °C; ^{1}H NMR (400 MHz, DMSO-d_6): δ 1.76 (s, 12H), 2.17 (t, J = 7.2 Hz, 4H), 3.13 (s, 18 H), 3.65 (tt, J = 7.6 Hz, J = 7.2 Hz, 4H), 4.27 (t, J = 7.6 Hz, 4H), 6.34 (d, J = 13.6 Hz, 2H), 7.51 (d, J = 8.4 Hz, 2H), 7.70 (d, J = 8.4 Hz, 2H), 7.93 (s, 2H), 8.73 (d, J = 13.6 Hz, 2H); ^{13}C NMR (100 MHz, DMSO-d_6), δ: 20.7, 26.4, 41.3, 49.7, 52.3, 62.1, 100.3, 113.3, 123.2, 123.5, 128.3, 130.0, 140.5, 143.4, 148.4, 174.3. Composition in theory: (x3H_2O): C (46.63%), H (6.13%), N (5.88%); Composition found: C (46.22%), H (6.12%), N (5.78%); HRMS (ESI) calculated for $[C_{37}H_{52}Cl_3BrN_4]^+$ m/z 736.2441, found m/z 736.2468.

5.1.3.9. 5-Bromo-2-((1E,3Z,5E)-3-bromo-5-(5-bromo-3,3-dimethyl-1-(3-(trimethylammonio)propyl)indolin-2-ylidene)penta-1,3-dien-1-yl)-3,3-dimethyl-1-(3-(trimethylammonio)propyl)-3H-indol-1-ium bromide (21). Yield 77.6%; Mp 232–234 °C; ^{1}H NMR (400 MHz, DMSO-d_6): δ 1.76 (s, 12H), 2.18 (t, J = 7.1 Hz, 4H), 3.12 (s, 18H), 3.55–3.65 (m, 4H), 4.24 (t, J = 7.0 Hz, 4H), 6.34 (d, J = 13.2 Hz, 2H), 7.60 (d, J = 8.6 Hz, 2H), 7.66 (d, J = 8.6 Hz, 2H), 8.06 (s, 2H), 8.60 (d, J = 13.2 Hz, 2H); ^{13}C NMR (400 MHz, DMSO-d_6), δ: 20.66, 26.46, 41.37, 49.79, 52.35, 62.25, 102.70, 113.74, 116.99, 118.22, 126.03, 131.24, 140.93, 143.72, 150.42, 174.34. Composition in theory: (3 × H_2O): C (40.91) H (5.38), N (5.16); Composition found: C (40.56), H (5.37), N (5.07). High-resolution electrospray ionization (ESI) accurate mass spectra calculated m/z for $[C_{37}H_{52}N_4Br_4]^+$ 868.0925, found 868.0930.

5.2. DNA and compound preparation

DNA oligonucleotides: Tel22, d[AGGG(TTAGGG)$_3$]; *c-myc*, d[(AGGGTGGGG)$_2$A]; control duplex, d[CGAATTCGTTTTCGAATTCG] with and without 5′-biotin labels were purchased from Integrated DNA Technologies (Coralville, IA) with HPLC purification. NMR and mass spectral analysis performed on these sequences further confirmed the purity. The concentration of oligonucleotides was determined from absorbance at 260 nm with extinction coefficients calculated by the nearest-neighbor method.[31] Appropriate stock solutions of the compounds were prepared in double deionized water and diluted with the experimental buffer prior to use.

Experiments were performed in 10 mM HEPES buffer containing 50 mM KCl and 3 mM EDTA adjusted to pH 7.3 using 1 N HCl.

5.3. UV-thermal melting studies

Thermal denaturation studies were conducted on a Cary 300 BIO UV–visible spectrophotometer in quartz cuvettes of 1 cm pathlength. DNA solutions were prepared at single-strand concentrations in the range of 2–3 μM in HEPES buffer. Samples of compound to DNA ratios ranging from 0:1 to 6:1 was prepared. The absorbance of the oligonucleotides and the complexes was monitored at the recommended wavelength of 295 nm for Tel22 and 260 nm for duplex DNA sequences as a function of temperature. Cuvettes were mounted in a thermal block, and the solution temperatures were monitored by a thermistor in a reference cuvette with computer-controlled heating and cooling rates of 0.5 °C/min. A total of four scans were collected (two heating and two cooling ramps). Data were analyzed and plotted using Kaleidagraph 4.0 software.

5.4. Circular dichroism

CD spectra were recorded using a Jasco J-810 spectrophotometer with a 1-cm pathlength quartz cuvette at a scan speed of 50 nm/min and response time of 1 s over the wavelength range of 230 nm to 700 nm. Quadruplex–DNA solutions (4–5 μM) were annealed overnight prior to the collection of spectra. Appropriate amount of ligands were sequentially titrated from the stock solution into the DNA solution in the cuvette until the desired mole ratios of compound to quadruplex were obtained. The spectra were averaged over four scans. A buffer scan was collected in the same cuvette and subtracted from the average scan of each ratio. Data were processed and plotted using Kaleidagraph 4.0 software.

5.5. Surface plasmon resonance

Biosensor-SPR experiments were performed with a four-channel Biacore 2000 optical biosensor system (GE Healthcare, Sweden). The streptavidin-derivatized gold chip (SA chip from BIAcore) was prepared for use by conditioning with a series of 60 s injections of 1 M NaCl in 50 mM NaOH followed by extensive washing with buffer. Biotinylated DNA samples (25–50 nM) in HEPES buffer were immobilized on the flow cell surface by non-covalent capture as previously described.[32] Flow cell 1 was left blank as a reference, while flow cells 2–4 were immobilized with 5′-biotinylated DNA by manual injection of DNA stock solutions (flow rate of 1 μL/min) until the desired amount of DNA response units was obtained (350–400 RU). Typically, a series of different ligand concentrations (1 nM to 1 μM) were injected onto the chip (flow rate of 25 μL/min, 5 min) until a constant steady-state response was obtained followed by a dissociation period (running buffer, 5 min). After every cycle, the chip surface was regenerated with 10 mM glycine solution (pH 2.5 for 30 s) followed by multiple buffer injections to obtain a stable baseline for following cycles.

The observed response (RU_{obs}) in the steady-state region is proportional to the amount of bound drug and was typically determined by linear averaging over 10–20 s or longer time span. The predicted maximum response per bound compound ($RU_{max/ligand}$) was calculated from the DNA molecular weight, the compound molecular weight, the amount of DNA immobilized on the flow cell, and the refractive index gradient ratio of the compound and DNA, as previously described.[32,33] The $RU_{max/ligand}$ value is required to convert RU_{obs} to determine the moles of drug bound to DNA. The RU_{obs} was plotted as a function of free ligand concentration (C_{free}) and the equilibrium binding constants were determined using a two-site interaction model, $RU_{max/ligand}(K_1C_{free} + 2K_1K_2C_{free}^2)/(1+K_1C_{free} + K_1K_2C_{free}^2)$ using nonlinear least-squares optimization to obtain an optimal fit with BIAevaluation (BIAcore Inc.) and Kaleidagraph (Synergy Software) softwares. K_1 and K_2 are equilibrium binding constants for two types of binding sites.

5.6. Isothermal titration calorimetry

ITC experiments were performed with a VP-ITC instrument (MicroCal, Northampton, MA). Calorimetric titrations were conducted by injecting 10 μL of the ligand (200 μM in Tris/K+ buffer) into the quadruplex solutions (20 μM in Tris/K+ buffer) every 300 s for a total of 29 injections. Similar experiments were performed to determine the heats of dilution of the ligand with buffer. The heat produced for each injection of compound into DNA or buffer was obtained by integration of the area under each peak of the titration plots with respect to time. The heats of reaction were obtained by subtraction of the integrated heats of dilution of the compounds from the heats corresponding to the injection of compound into DNA. Averaged subtraction was applied to ITC titration data. Data corresponding to the first injection were discarded. The binding enthalpy (ΔH) for each titration was obtained by fitting the results of heat per mole as a function of total molar ratio using a single-site binding model. The data was analyzed by VPViewer 2000 and Origin 7.0 software.

5.7. Mass spectrometry

The mass spectrometry analysis was performed on a Waters Q-TOF micromass spectrometer equipped with electrospray ionization source (ESI) in negative mode (Waters Corporate, Milford, MA). The mass range was from 500–3000 Da (displayed range in Fig. 5 is from 1100–2100 m/z). Since mass spectrometry generally requires DNA sequences dissolved in a volatile salt solution, all the sequences tested with mass spectrometry were dialyzed several times with a 1000 Da cut-off membrane (Spectrum Laboratories Inc., Rancho Dominguez, CA, USA) in 50 mM ammonium acetate buffer at pH 7.2 in order to remove any low molecular weight impurities from DNA. The final concentrations of the dialyzed DNA were determined as above (Section 5.2). Samples containing 25–30 μM *c-myc* sequence and appropriate amounts of ligands in the desired molar ratios to DNA were prepared in 50 mM ammonium acetate buffer with the final volume of 100 μL. The samples were introduced into the ion source through direct infusion at 5 μl/min flow rate. The instrument parameters were as follows: capillary voltage of 2200 V, sample cone voltage of 30 V, extraction cone voltage of 2.5 V, desolvation temperature of 70 °C and source temperature of 100 °C. Nitrogen was used as nebulizing and drying gas. Spectra were collected for 10 min and the last two minutes of the scan were used for data analysis. Data analysis and interpretation were performed using MassLynx 4.1 software.

Acknowledgments

The biophysical studies on cyanine-DNA interactions were supported by NIH NIAID Grant AI-064200 (WDW). The compound synthesis for this study was supported by a Georgia Research Alliance grant (MH). EAO was supported through internal funds from the Research Initiation and Mentor Grants at GSU and MH appreciates the Georgia State University Center for Diagnostics and Therapeutics for their support.

Supplementary data

Supplementary data associated with this article can be found, in the online version, at http://dx.doi.org/10.1016/j.bmc.2012.10.008.

References and notes

1. Neidle, S.; Balasubramanian, S. *Quadruplex nucleic acids*; RSC Pub: Cambridge, 2006.
2. Neidle, S.; Parkinson, G. N. *Biochimie* **2008**, *90*, 1184.
3. Neidle, S.; Thurston, D. E. *Nat. Rev. Cancer* **2005**, *5*, 285.
4. Han, H.; Hurley, L. *Trends Pharmacol. Sci.* **2000**, *21*, 136.
5. Drygin, D.; Siddiqui-Jain, A.; O'Brien, S.; Schwaebe, M.; Lin, A.; Bliesath, J.; Ho, C. B.; Proffitt, C.; Trent, K.; Whitten, J. P.; Lim, J. K. C.; Von Hoff, D.; Anderes, K.; Rice, W. G. *Cancer Res.* **2009**, *69*, 7653.
6. Monchaud, D. *Org. Biomol. Chem.* **2008**, *6*, 627.
7. Shi, D. F.; Wheelhouse, R. T.; Sun, D.; Hurley, L. H. *J. Med. Chem.* **2001**, *44*, 4509.
8. White, E. W.; Tanious, F.; Ismail, M. A.; Reszka, A. P.; Neidle, S.; Boykin, D. W.; Wilson, W. D. *Biophys. Chem.* **2007**, *126*, 140.
9. Henary, M.; Mojzych, M. In *Heterocyclic Polymethine Dyes: Synthesis, Properties and Applications*; Strekowski, L., Ed.; Springer: Berlin, 2008; Vol. 14, p 221.
10. Mojzych, M.; Henary, M. In *Heterocyclic Polymethine Dyes: Synthesis, Properties and Applications*; Strekowski, L., Ed.; Springer: Berlin, 2008; Vol. 14, p 1.
11. Yang, Q.; Xiang, J.; Yang, S.; Zhou, Q.; Li, Q.; Tang, Y.; Xu, G. *Chem. Commun.* **2009**, 1103.
12. Kerwin, S. M.; Sun, D.; Kern, J. T.; Rangan, A.; Thomas, P. W. *Bioorg. Med. Chem. Lett.* **2001**, *11*, 2411.
13. Rodger, A.; Norden, B. *Circular Dichroism and Linear Dichroism*; University Press: New York, Oxford, 1997.
14. Nanjunda, R.; Musetti, C.; Kumar, A.; Ismail, M. A.; Farahat, A. A.; Wang, S.; Sissi, C.; Palumbo, M.; Boykin, D. W.; Wilson, W. *Curr. Pharm. Des.* **1934**, *2012*, 18.
15. Munde, M.; Kumar, A.; Nhili, R.; Depauw, S.; David-Cordonnier, M.-H.; Ismail, M. A.; Stephens, C. E.; Farahat, A. A.; Batista-Parra, A.; Boykin, D. W.; Wilson, W. D. *J. Mol. Biol.* **2010**, *402*, 847.
16. Paramasivan, S.; Rujan, I.; Bolton, P. H. *Methods* **2007**, *43*, 324.
17. Rezler, E. M.; Seenisamy, J.; Bashyam, S.; Kim, M.-Y.; White, E.; Wilson, W. D.; Hurley, L. H. *J. Am. Chem. Soc.* **2005**, *127*, 9439.
18. Phan, A. T.; Kuryavyi, V.; Patel, D. J. *Curr. Opin. Struct. Biol.* **2006**, *16*, 288.
19. Hurley, L.; Wheelhouse, R.; Sun, D.; Kerwin, S.; Salazar, M.; Fedoroff, O.; Han, F.; Han, H.; Izbicka, E.; Von Hoff, D. *Pharmacol. Ther.* **2000**, *85*, 141.
20. Buchini, S.; Buschiazzo, A.; Withers, S. G. *Angew. Chem., Int. Ed.* **2008**, *47*, 2700.
21. Maehr, H. *Bioorg. Med. Chem.* **1997**, *5*, 473.
22. Chessari, G.; Woodhead, A. J. *Drug Discovery Today* **2009**, *14*, 668.
23. Hernandes, M. Z.; Cavalcanti, S. M.; Moreira, D. R.; Azevedo, F.; Leite, A. C. *Curr. Drug Targets* **2010**, *11*, 303.
24. Gray, R. D.; Li, J.; Chaires, J. B. *J. Phys. Chem. B.* **2009**, *113*, 2676.
25. Petraccone, L.; Garbett, N. C.; Chaires, J. B.; Trent, J. O. *Biopolymers* **2010**, *93*, 533.
26. Dai, J.; Carver, M.; Yang, D. *Biochimie* **2008**, *90*, 1172.
27. Garner, T. P.; Williams, H. E. L.; Gluszyk, K. I.; Roe, S.; Oldham, N. J.; Stevens, M. F. G.; Moses, J. E.; Searle, M. S. *Org. Biomol. Chem.* **2009**, *7*, 4194.
28. Kim, M.-Y.; Gleason-Guzman, M.; Izbicka, E.; Nishioka, D.; Hurley, L. H. *Cancer Res.* **2003**, *63*, 3247.
29. Debray, J.; Zeghida, W.; Jourdan, M.; Monchaud, D.; Dheu-Andries, M.-L.; Dumy, P.; Teulade-Fichou, M.-P.; Demeunynck, M. *Org. Biomol. Chem.* **2009**, *7*, 5219.
30. Peng, X.; Yang, Z.; Wang, J.; Fan, J.; He, Y.; Song, F.; Wang, B.; Sun, S.; Qu, J.; Qi, J.; Yan, M. *J. Am. Chem. Soc.* **2011**, *133*, 6626.
31. Fasman, G. D. *Handbook of Biochemistry and Molecular Biology, Nucleic Acids*; CRC Press: Cleveland, 1975.
32. Nanjunda, R.; Munde, M.; Liu, Y.; Wilson, W. In *Methods for Studying Nucleic Acid/Drug Interactions*; Tor, Y., Wanunu, M., Eds.; CRC Press: Boca Raton, 2011; p 91.
33. Davis, T. M.; Wilson, W. D. *Anal. Biochem.* **2000**, *284*, 348.